

Rapid thermal annealing effects on the structural properties and density of defects in SiO₂ and SiN_x:H films deposited by electron cyclotron resonance

E. San Andrés, A. del Prado, F. L. Martínez, I. Mártel, D. Bravo, and F. J. López

Citation: *Journal of Applied Physics* **87**, 1187 (2000); doi: 10.1063/1.371996

View online: <http://dx.doi.org/10.1063/1.371996>

View Table of Contents: <http://scitation.aip.org/content/aip/journal/jap/87/3?ver=pdfcov>

Published by the [AIP Publishing](#)



Re-register for Table of Content Alerts

Create a profile.



Sign up today!



Rapid thermal annealing effects on the structural properties and density of defects in SiO₂ and SiN_x:H films deposited by electron cyclotron resonance

E. San Andrés, A. del Prado, F. L. Martínez, and I. Mártil^{a)}

Departamento de Física Aplicada III, Facultad de Ciencias Físicas, Universidad Complutense de Madrid, E-28040 Madrid, Spain

D. Bravo and F. J. López

Departamento de Física de Materiales, Facultad de Ciencias, C-IV, Universidad Autónoma de Madrid, E-28049 Madrid, Spain

(Received 27 July 1999; accepted for publication 19 October 1999)

The effect of rapid thermal annealing processes on the properties of SiO_{2.0} and SiN_{1.55} films was studied. The films were deposited at room temperature from N₂ and SiH₄ gas mixtures, and N₂, O₂, and SiH₄ gas mixtures, respectively, using the electron cyclotron resonance technique. The films were characterized by Fourier transform infrared spectroscopy (FTIR) and electron paramagnetic resonance spectroscopy. According to the FTIR characterization, the SiO_{2.0} films show continuous stress relaxation for annealing temperatures between 600 and 1000 °C. The properties of the films annealed at 900–1000 °C are comparable to those of thermally grown ones. The density of defects shows a minimum value for annealing temperatures around 300–400 °C, which is tentatively attributed to the passivation of the well-known *E'* center Si dangling bonds due to the formation of Si–H bonds. A very low density of defects ($5 \times 10^{16} \text{ cm}^{-3}$) is observed over the whole annealing temperature range. For the SiN_{1.55} films, the highest structural order is achieved for annealing temperatures of 900 °C. For higher temperatures, there is a significant release of H from N–H bonds without any subsequent Si–N bond healing, which results in degradation of the structural properties of the film. A minimum in the density of defects is observed for annealing temperatures of 600 °C. The behavior of the density of defects is governed by the presence of non-bonded H and Si–H bonds below the IR detection limit. © 2000 American Institute of Physics. [S0021-8979(00)05903-X]

I. INTRODUCTION

Silicon oxide (SiO₂) and silicon nitride (SiN_x:H) are the most extensively used dielectrics in the microelectronics industry. The Si/SiO₂ system is characterized by excellent interface and electrical properties. However, as the scale of integration increases and the thickness of the dielectric is reduced, the performance of SiO₂ is degraded due to tunneling currents and permeability to boron and alkali ion diffusion. SiN_x:H shows better impermeability properties than SiO₂, as well as a higher dielectric constant which allows physically thicker dielectrics with the same capacitance–voltage performance.¹ Different approaches have been developed to combine the properties of SiO₂ and SiN_x:H, such as stacked oxide–nitride–oxide (ONO) structures,² nitrided silicon oxide films,³ or compound silicon oxinitride films.^{1,4} Additionally, research is being devoted to the application of SiN_x:H as the gate dielectric in III–V based metal–insulator–semiconductor field effect transistors (MISFETs).^{5,6}

The requirements of ultralarge scale integration (ULSI) technology have stimulated the development of low thermal budget processes for the deposition of device quality SiO₂ and SiN_x:H. Plasma-enhanced chemical vapor deposition (PECVD) techniques are of great interest as they make use of a plasma for the generation of active precursor species which

allows the deposition of the films at low temperatures. In particular, the electron cyclotron resonance (ECR) technique shows some interesting features in addition to the low thermal budget requirement. A very efficient activation of the precursor gases can be achieved, allowing the use of N₂ instead of NH₃ as the N atom source, which results in lower incorporation of hydrogen into the films.^{7,8} Additionally, the damage due to ion bombardment is reduced, since the substrates are placed outside the plasma region.⁹

However, plasma deposited films show worse electrical properties than thermally grown ones. Rapid thermal annealing (RTA) post-deposition processes have been found to improve the performance of plasma deposited dielectrics, as the thermal relaxation of the lattice is induced while the low thermal budget requirement is satisfied.^{2–4,10–13}

In this work, the influence of RTA processes on the bonding properties and density of defects in SiO₂ and SiN_x:H films deposited by the ECR plasma technique are analyzed and compared.

Fourier transform infrared spectroscopy (FTIR) was employed in order to characterize the bonding and structural properties of the films. This technique provides information on the different bonds present in the film, which show characteristic absorption bands, as well as information regarding the structural order, since the width of these bands is related to the different bonding environments.¹⁴

^{a)} Author to whom correspondence should be addressed; electronic mail: imartil@eucmax.sim.ucm.es

The density of defects was studied by electron paramagnetic resonance (EPR). This technique has proven to be a powerful tool for the detection of characteristic defects in amorphous $\text{SiN}_x\text{:H}$ (K and N centers)¹⁵ and SiO_2 (E' and P_b centers).^{16,17}

II. EXPERIMENT

All samples were deposited using an Astex ECR plasma source, model AX-4500, attached to an in-house designed deposition chamber, pumped by a turbomolecular pump. Details of the deposition system are given elsewhere.¹⁸ $\text{SiN}_x\text{:H}$ films were deposited from N_2 and SiH_4 mixtures, with a N_2/SiH_4 ratio of 7.5, while silicon oxide films were deposited from N_2 , O_2 , and SiH_4 mixtures, with $\text{O}_2/\text{SiH}_4=4.5$ and $(\text{N}_2+\text{O}_2)/\text{SiH}_4=9.1$. For all depositions, the total gas flow, pressure, and microwave power were kept constant at 10.5 sccm, 0.7 mTorr, and 100 W, respectively. Substrates were not intentionally heated and the deposition temperature was estimated to be about 50 °C. The composition of the nitride films was previously determined by Rutherford backscattering to be $x=1.55$.¹⁹ Auger electron spectroscopy measurements performed on the oxide films indicated that the samples consisted of $\text{SiO}_{2.0}$, with no detectable incorporation of nitrogen.²⁰

High resistivity (80 Ω cm p -type Si(111) wafers polished on both sides were used as substrate for all samples. The substrates were cleaned by using standard chemical procedures.¹⁹ After deposition of the dielectric, several 1×1 cm samples were cut from the same deposited film to perform RTA processes at different temperatures, so that all samples in a series were deposited under the same conditions. As-deposited, nonannealed samples were also saved to use as a reference. The thickness of the films was about 300 nm for FTIR characterization, while a stack of five films with a total dielectric thickness of 1.5–3 μm was used for the EPR measurements.

RTA processes were performed in a Modular Process Technology furnace, model RTP-600, equipped with a graphite susceptor. Samples were annealed at temperatures ranging between 300 and 1050 °C for 30 s in an argon atmosphere.

FTIR spectroscopy was performed using a Nicolet Magna-IR 750 series II spectrometer working in the transmission mode at normal incidence. The N–H content of the silicon nitride films was determined from the N–H stretching band according to the method developed by Lanford and Rand.²¹ The spectrum of the deposited film was obtained by subtracting the substrate spectrum from the total signal (substrate+deposited film).

The EPR measurements were performed at room temperature using a Bruker ESP 300E X-band spectrometer at 0.5 mW power, which is low enough to prevent the saturation of the signal.

III. RESULTS AND DISCUSSION

A. FTIR spectroscopy

The FTIR spectra of the as-deposited SiO_2 films show the characteristic Si–O stretching, bending and rocking

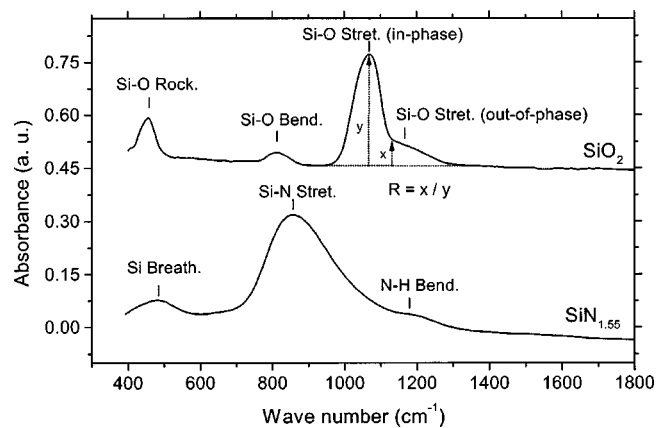


FIG. 1. FTIR spectra of SiO_2 and $\text{SiN}_{1.55}$ films.

bands, located at 1069, 814, and 457 cm^{-1} , respectively.²² No O–H or Si–H bands were detected. The Si–O stretching band can be decomposed in a sharp band centered near 1075 cm^{-1} , and a broad shoulder located around 1130–1150 cm^{-1} .^{22,23} These bands are attributed to the in-phase and out-of-phase motion of the oxygen atoms.²² The ratio of the shoulder height versus the height of the maximum (R) has been used to characterize the high frequency shoulder. As the O/Si ratio of the films decreases from the stoichiometric value (O/Si=2), a shift of the stretching band to lower wave numbers, as well as an increase in R has been reported, indicating that these parameters are related to the composition of the silicon oxide.²² All these characteristics are shown in Fig. 1 for the as-deposited SiO_2 films.

Figure 2 shows the wave number of the Si–O stretching band and the parameter R as a function of annealing temperature (T_a) for $\text{SiO}_{2.0}$ samples. The results are averaged over two different series, which show essentially the same values. For T_a up to 500 °C, there is no change in the wave number while R marginally decreases. When T_a increases from 500 to 1000 °C, the maximum of the band shifts to higher wave numbers up to 1080 cm^{-1} . A decrease of R from 0.27 to 0.23 is also observed when increasing T_a . The values of R reported in this work are lower than those reported in Ref. 22 for SiO_2 samples, but are similar to those reported by other authors for ECR deposited silicon oxide films.²⁴

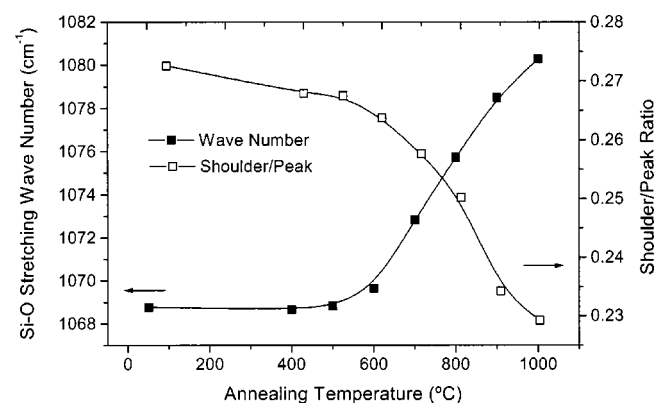


FIG. 2. Wave number and shoulder/peak ratio of the Si–O stretching band as a function of annealing temperature for $\text{SiO}_{2.0}$ samples.

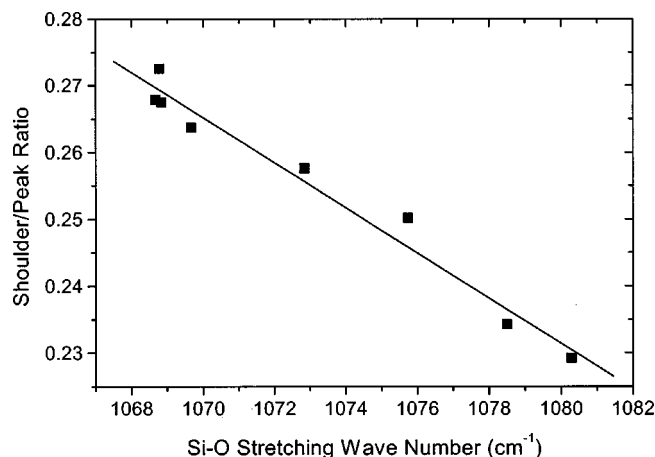


FIG. 3. Shoulder to peak ratio of the Si–O stretching band as a function of the wave number of the maximum.

The shift of the stretching band is unlikely to be correlated with changes in the composition of the films, since the as-deposited samples are already stoichiometric $\text{SiO}_{2.0}$. We attribute the increase in the frequency of the stretching band to an increase in the Si–O–Si bond angle. According to the central force model, the wave number or frequency of the Si–O stretching vibration is given by

$$v = v_0 \sin \theta, \quad (1)$$

where θ is half of the Si–O–Si bond angle and v_0 is empirically determined to be 1134 cm^{-1} assuming $\theta = 72^\circ$ for a fully relaxed thermally grown SiO_2 with $v = 1078.5 \text{ cm}^{-1}$.²⁵ This bond angle is also directly related to the distance between the Si atoms bonded to the O atom. Fitch *et al.* have shown that the Si–Si distance, or equivalently, the Si–O–Si bond angle or frequency of the Si–O stretching band can be related to the local atomic strain in the SiO_2 network which is proportional to the compressive stress in the film, so that as the frequency of the band approaches the thermal oxide value (1078.5 cm^{-1}), the stress decreases.²⁵

In our samples, as the annealing temperature increases above 500°C , there is a continuous increase in the Si–O stretching frequency from 1069 to 1080 cm^{-1} , which is explained by an increase in the bond angle as the relaxation of the lattice stress is induced. For annealing temperatures of 900 – 1000°C , the frequency of the stretching band is essentially the same as in thermally grown oxides, while the thermal budget of the process is significantly lower. Similar results have been reported by other authors for PECVD silicon oxide films,^{14,25} ECR deposited nitrided SiO_2 films³ and rf sputtered silicon oxide films,²⁶ and related to improvements in the electrical properties.^{3,26}

Together with the shift of the Si–O stretching band, a decrease in the parameter R is observed when increasing T_a . Figure 3 shows the shoulder/peak ratio R of the Si–O stretching band as a function of the wave number of the maximum. A linear correlation between these parameters is found, as shown in Fig. 3. Even when there is no change in the composition of the sample, the parameter R is still related to the frequency of the stretching band, and therefore, to the Si–O–Si bond angle and stress of the film.

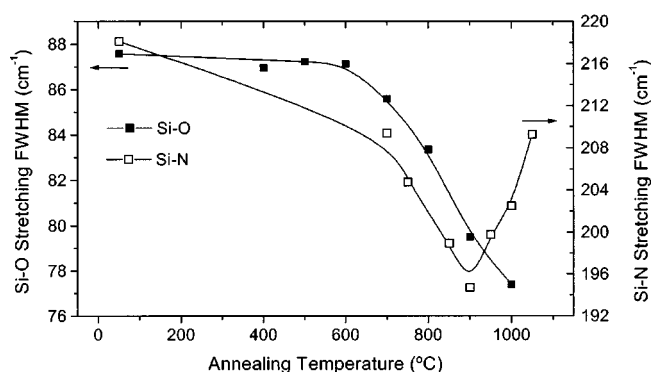


FIG. 4. FWHM of the Si–O stretching band of $\text{SiO}_{2.0}$ samples and FWHM of the Si–N stretching band of $\text{SiN}_{1.55}$ samples, as a function of annealing temperature.

The full width at half maximum (FWHM) of the Si–O stretching band as a function of T_a is shown in Fig. 4. This parameter is related to the statistical distribution of different bonding environments, so that a lower value of the FWHM means a lower dispersion of local environments and a higher structural order of the film.^{14,25} The FWHM of the $\text{SiO}_{2.0}$ films remains constant at about 87 cm^{-1} for T_a up to 600°C . As T_a is increased from this value, the FWHM decreases, together with an increase in the frequency of the maximum, until a value of 77 cm^{-1} for $T_a = 1000^\circ\text{C}$ is reached. This behavior reveals an improvement in the structural order of the film with increasing T_a . This result is very similar to that reported for ECR deposited nitrided silicon oxide films using N_2O as precursor gas instead of a mixture of N_2 and O_2 .³ It is important to mark the tight correlation between the FWHM and the frequency of the Si–O stretching band. The structural ordering evidenced by the decrease in FWHM takes place in the same T_a range (600 – 1000°C) as the decrease in the stress deduced from the shift of the peak to higher wave numbers.

The improvements in the $\text{SiO}_{2.0}$ properties obtained by RTA are better than those reported by our research group when increasing the deposition temperature up to 200°C .²⁷ In order to achieve as-deposited properties equivalent to those of annealed samples, higher deposition temperatures should be used, which may not satisfy the low thermal budget requirements of ULSI technology.

Figure 1 shows the low frequency range of the FTIR spectrum of as-deposited $\text{SiN}_{1.55}$ films. The spectrum shows a dominant band centered around 865 cm^{-1} with a small shoulder at 1175 cm^{-1} , and two small bands located around 480 and 3335 cm^{-1} . These features are characteristic of silicon nitride films and are attributed to Si–N stretching, N–H bending, Si breathing, and N–H stretching vibrations, respectively.²⁸ No Si–H bonds were detected, which is expected due to the high N/Si ratio of these samples (N/Si = 1.55).

As T_a is increased, there is no significant change in the position of the Si–N stretching band, but the FWHM is strongly affected, as shown in Fig. 4. As T_a is increased up to 900°C , there is a continuous decrease in the FWHM from 218 cm^{-1} to a minimum value of 194 cm^{-1} . For higher

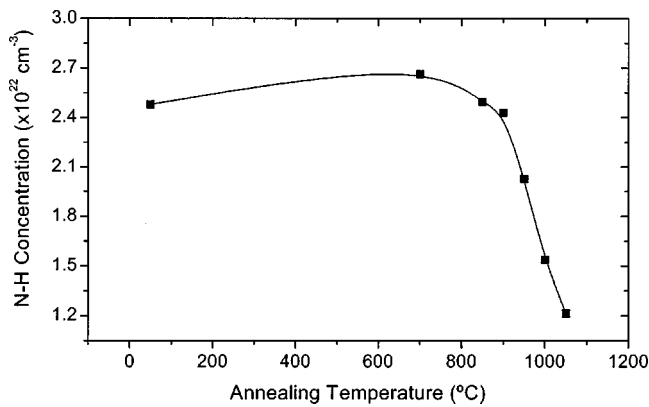
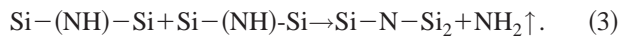
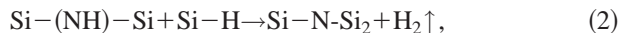


FIG. 5. N–H bond concentration as a function of annealing temperature for $\text{SiN}_{1.55}$ samples.

annealing temperatures, the FWHM further increases. The behavior of the $\text{SiN}_{1.55}$ films is different from that of SiO_2 films. While the SiO_2 structural properties improve over the whole annealing temperature range, there is an optimum T_a value ($T_a = 900^\circ\text{C}$) for the $\text{SiN}_{1.55}$ films; higher annealing temperatures result in degraded properties of the films.

Plasma-deposited silicon nitride films are characterized by the presence of significant amounts of H in the form of N–H and Si–H bonds and molecular and atomic nonbonded H. This H is known to have an important role in the thermal relaxation processes of the network.^{10,11,19,29,30}

Figure 5 shows the N–H bond concentration obtained from the FTIR measurements as a function of annealing temperature for the $\text{SiN}_{1.55}$ samples. For T_a up to 700°C , there is a slight increase in the N–H concentration. For temperatures between 700 and 900°C , the N–H content is roughly the same as in as-deposited films. Finally, for T_a above 900°C , there is a significant release of H due to the breaking of N–H bonds. The increase in the N–H content observed for moderate annealing temperatures can only be explained by the presence of nonbonded H which, in this temperature range, reacts to form new N–H bonds. The release of H induced by RTA is usually governed by overall network reactions involving both N–H and Si–H bonds. The following reactions have been proposed in the literature for plasma-deposited SiN_x :H films:²⁹



Reaction (2) implies formation of new Si–N bonds at the expense of the breaking of both Si–H and N–H bonds, followed by Si–N bond healing. This reaction is very unlikely to take place in the films studied in this work, since the Si–H concentration is below the detection limit. Additionally, no significant increase in the area of the Si–N stretching band is observed. Regarding reaction (3), this reaction implies the loss of N due to the formation of volatile NH_2 species. It has been shown in previous work¹⁹ that the annealing of our ECR deposited $\text{SiN}_{1.55}$ samples does not result in any N loss, so we conclude that reaction (3) does not occur or is negligible. Additionally, the increase in the FWHM observed for annealing temperatures above 900°C suggests a degradation

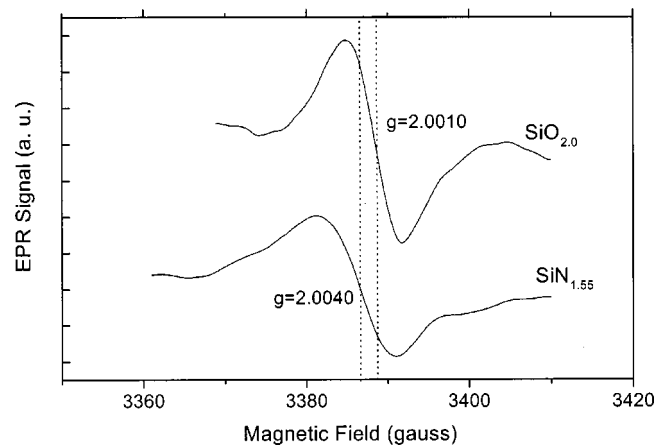
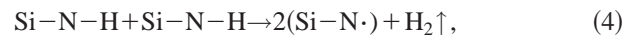


FIG. 6. EPR spectra for $\text{SiO}_{2.0}$ and $\text{SiN}_{1.55}$ films.

of the structural order of the lattice which may be associated with the breaking of the N–H bonds without Si–N bond healing. Samples of Ref. 29 were deposited using NH_3 while, in this work, N_2 was used. It is known that the use of N_2 instead of NH_3 reduces the incorporation of H into the films.⁴ Reaction (3) requires the presence of near-neighbor SiN–H groups. The lower H content of our samples, when compared to those of Ref. 29, results in a lower density of neighbor SiN–H groups, so that the probability of reaction (3) taking place is low. The following reaction is proposed instead to explain the results obtained:



where $\text{N}\cdot$ is used to indicate that there is no Si–N bond healing after the breaking of the N–H bonds. This breaking of N–H bonds without subsequent bond healing accounts for the degradation of the lattice evidenced by the increase in the FWHM of the Si–N stretching band.

B. EPR results

Figure 6 shows the EPR signals for as-deposited SiO_2 and $\text{SiN}_{1.55}$ samples. The spectrum of the SiO_2 films shows a main feature for low g values, $g = 2.0010$ – 2.0020 . The most characteristic defects in SiO_2 films are the E' center¹⁶ and the P_b center.¹⁷ Low g values are characteristic of the E' center, so we conclude the observed signal is mainly due to this defect, although the exact kind of E' defect among all the possible types can not be identified.

The spectrum of the $\text{SiN}_{1.55}$ films shows a single peak centered around $g = 2.0040$. We attribute this signal to the K center. The exact location of the EPR signal for this center shifts from 2.0055 for $\cdot\text{Si}\equiv\text{Si}_3$ to 2.0028 for $\cdot\text{Si}\equiv\text{N}_3$.¹⁵ Given the high N/Si ratio of our samples, the $\cdot\text{Si}\equiv\text{N}_3$ configuration is the most probable one. The shift of g from the 2.0028 value is attributed to possible contributions of different defects, such as $\cdot\text{Si}\equiv\text{SiN}_2$ configurations, $\cdot\text{Si}\equiv\text{Si}_2\text{O}$ groups which may appear due to O contamination,³¹ or even the influence of N dangling bonds.³² Similar g values to those obtained in this work have been reported for high N/Si ratio silicon nitride films.³²

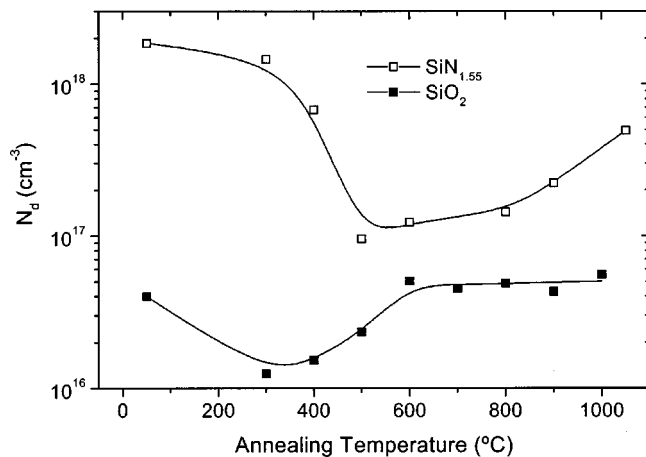


FIG. 7. Spin density for $\text{SiO}_{2.0}$ and $\text{SiN}_{1.55}$ samples as a function of annealing temperature.

Figure 7 shows the total spin density (N_d) as a function of annealing temperature (T_a) for both SiO_2 and $\text{SiN}_{1.55}$ films. The values for the SiO_2 films, which are lower and may be more affected by noise, are averaged over three different samples for each annealing temperature.

The $\text{SiN}_{1.55}$ spin density decreases as T_a increases up to 500–600 °C. The minimum value of N_d is about $1 \times 10^{17} \text{ cm}^{-3}$ and is obtained for $T_a = 500$ °C. For temperatures above 600 °C, N_d increases with respect to the minimum value.

The EPR results can be explained by taking into account the presence of nonbonded H, deduced from the increase in the N–H bond concentration. It has been shown in a previous paper that there is an increase in the Si–H bond concentration when increasing T_a up to 500 °C for silicon nitride samples with lower N/Si ratio values (N/Si=0.97).¹⁹ The observed decrease in N_d in the low annealing temperature range can be explained by the same mechanism also taking place in the samples of this work. The formation of Si–H bonds at the expense of nonbonded H results in a passivation of the EPR active Si dangling bonds, with a subsequent decrease in N_d . These Si–H bonds are not observed by FTIR because the concentration is below the detection limit. For T_a above 600 °C, there is a release of H from the Si–H bonds which accounts for the increase in N_d .

The optimum annealing temperature value, $T_a = 500$ °C, corresponding to the minimum in N_d deduced from EPR, is different from the value obtained by FTIR for the minimum of the FWHM and maximum structural order, which occur for $T_a = 900$ °C. It must be noted that the N_d values range around 10^{17} – 10^{18} cm^{-3} , which is orders of magnitude below the FTIR detection limit. So, the mechanisms responsible for the behavior of the EPR signal may not be detectable by FTIR. Furthermore, the FTIR results are related to structural relaxation processes, while the behavior of the EPR signal is explained by the passivation of Si dangling bonds. Therefore, the two measurements are not contradictory, but account for different mechanisms.

Concerning the SiO_2 samples, the behavior is similar to that observed for $\text{SiN}_{1.55}$, but there are some differences.

First, the SiO_2 total spin density is about one order of magnitude lower than for $\text{SiN}_{1.55}$, with values ranging around 2 – $5 \times 10^{16} \text{ cm}^{-3}$. As T_a increases, there is also a minimum in N_d for SiO_2 samples, but the corresponding temperature is about 300–400 °C instead of 500–600 °C as observed for $\text{SiN}_{1.55}$. Again, the EPR and FTIR measurements seem not to be correlated, since the FTIR results show a continuous relaxation up to 1000 °C. As previously discussed, EPR is significantly more sensitive than FTIR, allowing the detection of defects which may not have any effect on the FTIR spectrum. The behavior of the SiO_2 films is tentatively explained in a similar way as for $\text{SiN}_{1.55}$. The presence of H has been reported in ECR deposited SiO_2 films.³³ Our results can be explained by assuming the presence of H below the FTIR detection limit or nonbonded H. As T_a increases, this H can passivate Si dangling bonds while, for $T_a = 600$ °C, this H is released and the spin density becomes the same as in as-deposited films. It must be noted that very low N_d values are observed over the whole annealing temperature range.

The effect of RTA on the electrical properties of $\text{SiN}_{1.55}$ samples has been studied in detail in a previous paper.¹⁰ In that work, it was found that the minimum in N_d was correlated with the minimum in the density of interfacial states, D_{it} , and with the best resistivity and breakdown field values. However, this conclusion can not be directly extended to SiO_2 films, since the H content plays a key role in the properties of $\text{SiN}_{1.55}$ films and the H content of the SiO_2 films is significantly lower. Improvements in the electrical properties of silicon oxide films have been reported for annealing temperatures around 1000 °C.^{3,26} These improvements are related to the thermal relaxation of the lattice observed for these high annealing temperatures. However, the minimum in N_d observed in this work for $T_a = 300$ – 400 °C, together with the relationship between N_d and the electrical properties, suggests the possibility of low annealing temperatures as an alternate method to improve the performance of SiO_2 films.

IV. SUMMARY

The effect of RTA processes on the bonding structure and density of defects in $\text{SiO}_{2.0}$ and $\text{SiN}_{1.55}$ films was analyzed. The films were deposited at room temperature using the ECR plasma technique. For the $\text{SiO}_{2.0}$ films, a thermal relaxation of the lattice and stress relief is observed over the whole annealing temperature range between 600 and 1000 °C. The characteristics of the IR spectrum for samples annealed between 900 and 1000 °C are essentially the same as thermally grown oxides and are better than those obtained for nonannealed films deposited at 200 °C. Concerning the EPR results, a minimum in the density of defects is observed for annealing temperatures between 300 and 400 °C. This behavior is attributed to the passivation of defects by the formation of Si–H bonds from the nonbonded H present in the film. These results suggest the possibility of low temperature annealing processes for improvement in the quality of SiO_2 films.

For the $\text{SiN}_{1.55}$ films, an improvement in the structural order is observed for annealing temperatures up to 900 °C. For higher annealing temperatures, the release of H due to the breaking of N–H bonds results in degradation of the properties of the film. The density of defects is correlated to the H content of the films. For temperatures up to 600 °C, there is an increase in the N–H bond concentration and a decrease in the density of defects, which is again explained by the formation of Si–H bonds. For higher annealing temperatures, the release of H results in an increase in the density of defects. It is concluded that the H content plays a key role in the thermal stability of the SiN_x :H films.

ACKNOWLEDGMENTS

The authors acknowledge C. A. I. de Implantación Iónica (U. C. M.) for technical support and C. A. I. de Espectroscopía (U. C. M.) for availability of the FTIR spectrometer. The work has been financed by the CICYT (Spain) under Contract No. TIC 98/0740.

- ¹Y. Ma and G. Lukovsky, *J. Vac. Sci. Technol. B* **12**, 2504 (1994).
- ²Y. Ma, T. Yasuda, and G. Lukovsky, *J. Vac. Sci. Technol. B* **11**, 1533 (1993).
- ³D. Landheer, Y. Tao, J. E. Hulse, T. Quance, and D.-X. Xu, *J. Electrochem. Soc.* **143**, 1681 (1996).
- ⁴S. V. Hattangady, H. Niimi, and G. Lucovsky, *J. Vac. Sci. Technol. A* **14**, 3017 (1996).
- ⁵E. Redondo, N. Blanco, I. Mártil, and G. González-Díaz, *Appl. Phys. Lett.* **74**, 991 (1999).
- ⁶D. G. Park, M. Tao, D. Li, A. E. Botchkarev, Z. Fan, Z. Wang, S. N. Mohammad, A. Rockett, J. R. Abelson, H. Morkoç, A. R. Heyd, and S. A. Alterovitz, *J. Vac. Sci. Technol. B* **14**, 2674 (1996).
- ⁷P. K. Shufflebotham, D. J. Thomson, and H. C. Card, *J. Appl. Phys.* **64**, 4398 (1988).
- ⁸A. Popov, *J. Vac. Sci. Technol. A* **7**, 894 (1989).
- ⁹T. T. Chau, S. R. Mejia, and K. C. Kao, *J. Vac. Sci. Technol. B* **10**, 2170 (1992).
- ¹⁰F. L. Martínez, A. del Prado, D. Bravo, F. López, I. Mártil, and G. González-Díaz, *J. Vac. Sci. Technol. A* **17**, 1280 (1999).
- ¹¹G. Lucovsky, H. Niimi, Y. Wu, C. R. Parker, and J. R. Hauser, *J. Vac. Sci. Technol. A* **16**, 1721 (1998).
- ¹²D. Landheer, J. E. Hulse, and T. Quance, *Thin Solid Films* **293**, 52 (1997).
- ¹³N. Bhat, A. W. Wang, and K. C. Saraswat, *IEEE Trans. Electron Devices* **46**, 63 (1999).
- ¹⁴A. Sassella, A. Borghesi, F. Corni, A. Monelli, G. Ottaviani, R. Tonini, B. Pivac, M. Bacchetta, and L. Zanotti, *J. Vac. Sci. Technol. A* **15**, 377 (1997).
- ¹⁵W. L. Warren, J. Kanicki, F. C. Rong, and E. H. Poindexter, *J. Electrochem. Soc.* **139**, 880 (1992).
- ¹⁶W. L. Warren, E. H. Poindexter, M. Offenber, W. Müller-Warmuth, *J. Electrochem. Soc.* **139**, 872 (1992).
- ¹⁷E. H. Poindexter, G. J. Gerardi, M.-E. Rueckel, P. J. Caplan, N. M. Johnson, and D. K. Biegelsen, *J. Appl. Phys.* **56**, 2844 (1984).
- ¹⁸S. García, J. M. Martín, M. Fernández, I. Mártil, and G. González-Díaz, *Philos. Mag. B* **73**, 487 (1996).
- ¹⁹F. L. Martínez, I. Mártil, G. González-Díaz, B. Selle, and I. Sieber, *J. Non-Cryst. Solids* **227-230**, 523 (1998).
- ²⁰A. del Prado, I. Mártil, M. Fernández, and G. González-Díaz, *Thin Solid Films* **343-344**, 432 (1999).
- ²¹W. A. Lanford and M. J. Rand, *J. Appl. Phys.* **49**, 2473 (1978).
- ²²P. G. Pai, S. S. Chao, Y. Takagi, and G. Lucovski, *J. Vac. Sci. Technol. A* **4**, 689 (1986).
- ²³B.-R. Zhang, Z. Yu, G. J. Collins, T. Hwang, and W. H. Ritchie, *J. Vac. Sci. Technol. A* **7**, 176 (1989).
- ²⁴T. V. Herak, T. T. Chau, D. J. Thomson, S. R. Mejia, D. A. Buchanan, and K. C. Kao, *J. Appl. Phys.* **65**, 2457 (1989).
- ²⁵J. T. Fitch, S. S. Kim, and G. Lucovsky, *J. Vac. Sci. Technol. A* **8**, 1871 (1990).
- ²⁶W. K. Choi, C. K. Choo, and Y. F. Lu, *J. Appl. Phys.* **80**, 5837 (1996).
- ²⁷A. del Prado, F. L. Martínez, M. Fernández, I. Mártil, and G. González-Díaz, *J. Vac. Sci. Technol. A* **17**, 1263 (1999).
- ²⁸D. V. Tsu, G. Lucovsky, and M. J. Mantini, *Phys. Rev. B* **33**, 7069 (1986).
- ²⁹Z. Lu, P. Santos-Filho, G. Stevens, M. J. Williams, and G. Lucovsky, *J. Vac. Sci. Technol. A* **13**, 607 (1995).
- ³⁰R. C. Budhani, R. F. Bunshah, and P. A. Flinn, *Appl. Phys. Lett.* **52**, 284 (1988).
- ³¹S. García, D. Bravo, M. Fernández, I. Mártil, and F. J. López, *Appl. Phys. Lett.* **67**, 3263 (1995).
- ³²D. Jousse, J. Kanicki, D. T. Krick, and P. M. Lenahan, *Appl. Phys. Lett.* **52**, 445 (1988).
- ³³J. K. Cramer and S. P. Murarka, *J. Appl. Phys.* **77**, 3048 (1995).